

ELECTRONIC SUPPLEMENTARY INFORMATION

Electrochemical performance of cobalt hydroxide nanosheets formed by the delamination of layered cobalt hydroxide in water

Barbora Schneiderová,^{a,b} Jan Demel,^a Josef Pleštil,^c Hana Tarábková,^d Jan Bohuslav,^{d,e} and Kamil Lang^{*a}

^a *Institute of Inorganic Chemistry of the AS CR, v. v. i., Husinec-Řež 1001, 250 68 Řež, Czech Republic*

^b *Faculty of Science, Charles University in Prague, Hlavova 2030, 128 43 Praha 2, Czech Republic*

^c *Institute of Macromolecular Chemistry of the AS CR, v. v. i., Heyrovského nám. 2, 162 06 Praha 6, Czech Republic*

^d *J. Heyrovský Institute of Physical Chemistry of the AS CR, v. v. i., Dolejškova 3, 182 23 Praha 8, Czech Republic*

^e *Institute of Chemical Technology, Prague, Technická 5, 166 28 Praha 6, Czech Republic*

*Corresponding author: Email address: lang@iic.cas.cz, Tel: +420 26617 2193, Fax: +420 22094 1502.

Contents

- Table S1. Conditions of syntheses and characterizing data of LCoH-DS.
- Table S2. Charge reversibility of the LCoH-Lactate electrodes.
- Figure S1. Powder XRD patterns of LCoH-DS.
- Figure S2. FTIR spectra of LCoH-DS and LCoH-Lactate.
- Figure S3,S4. Thermal analyses of LCoH-DS and LCoH-Lactate.
- Figure S5. UV/vis absorption spectrum of the LCoH-Lactate colloid and self-standing film.
- Figure S6,S7. SAXS curves of the aqueous dispersions.
- Figure S8. AFM amplitude image (tapping mode) of the drop-casted deposit on the basal plane HOPG.
- Figure S9. Dependence of the peak current *vs.* potential scan rate (ν) for the spin-coated cobalt hydroxide deposits on the basal plane HOPG.
- Figure S10. Dependence of the peak potential *vs.* potential scan rate (ν) for the spin-coated cobalt hydroxide deposits on the basal plane HOPG.
- Figure S11. Cyclic voltammetry of the spin-coated cobalt hydroxide deposits on the basal plane HOPG.

Table S1. Conditions of syntheses and characterizing data of LCoH-DS.

Sample	HMT/eq	T/°C	Time/h	Solvent	d / Å	Colour	Molar ratio Co/DS ^b
1	20	90	2	H ₂ O,MeOH	24.1	green	0.30
2	20	90	2	H ₂ O,BuOH	19.5	beige	0.25
3	20	90	1	H ₂ O,BuOH	22.6	beige	0.27
4	10	90	2	H ₂ O,BuOH	19.9	beige	0.25
5	3	90	2	H ₂ O,BuOH	23.1	green	0.27
6 ^a	3	100	24	H ₂ O	26.1	green	0.28

^a Reaction was performed in an autoclave.

^b Composition of synthesized LCoH-DS was estimated using elemental analyses data; molar ratio of Co/HMT was 1/0.04.

Table S2. Charge reversibility expressed as the ratio of anodic (Q_a) and cathodic (Q_c) charges (Q_a/Q_c) was elucidated from cyclic voltammograms of the spin-coated cobalt hydroxide electrodes vs. potential scan rate (v).

$v/\text{mV s}^{-1}$	Q_a/Q_c^a	Q_a/Q_c^b
10	1.01	1.01
20	0.75	1.23
50	0.78	0.88
100	0.77	0.87
200	0.93	0.84

^a Deposit prepared by spin-coating using the 10 mg ml⁻¹ dispersion.

^b Deposit prepared by spin-coating using the 2 mg ml⁻¹ dispersion.

Figure S1. Examples of powder XRD patterns recorded for LCoH-DS **6** (a) and LCoH-DS **4** (b). The sample LCoH-DS **6** has a minor contribution of a more extended phase with a basal spacing of 33.6 Å (●).

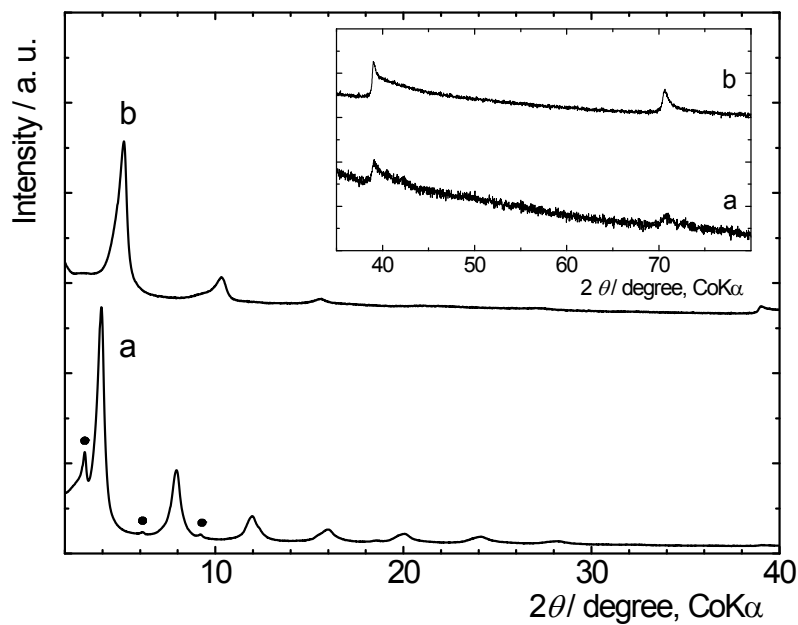
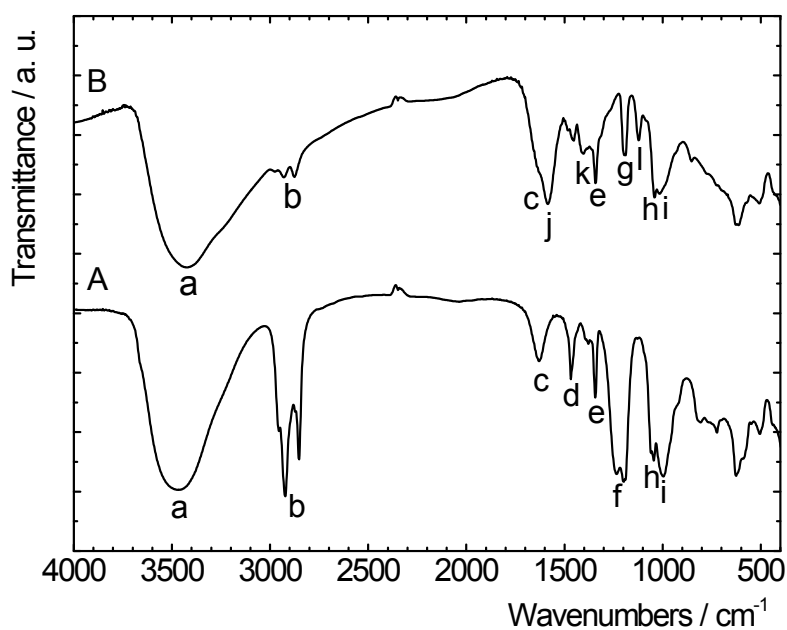


Figure S2. FTIR spectra of LCoH-DS **4** (A) and LCoH-Lactate (B). The spectra are vertically shifted and labelling refers to the discussion below.



FTIR spectra of LCoH-DS and LCoH-Lactate display vibrations of the intercalated anions, water molecules (the OH stretching vibrations at approximately 3440 cm^{-1} (a) and the OH deformation vibration at 1633 cm^{-1} (c)), and the skeletal vibrations of cobalt hydroxide (below 1000 cm^{-1}). Intercalated DS anions display the stretching vibrations of the C-H bonds in the range $3000 - 2780\text{ cm}^{-1}$ (b), the bending vibration of the organic chain at 1468 cm^{-1} (d), and the sulphate vibrations at 1234 and 1200 (f), 1045 (h), and 997 cm^{-1} (i). The traces of remaining HMT are indicated by the vibration at 1341 cm^{-1} (e), the other bands overlap with the signals of the sulphate groups.

Anion exchange of DS with the lactate anion is accompanied by the appearance of the stretching C-OH vibrations at 1120 cm^{-1} (l) and the asymmetric and symmetric stretching modes of the lactate carboxyl group at 1587 cm^{-1} (j) and 1405 cm^{-1} (k), respectively. The peaks at 2929 cm^{-1} and 2875 cm^{-1} (b), 1189 cm^{-1} (g), and the peaks (h, i) indicate the minor presence of HMT and DS, as was also confirmed by elemental analyses.

Figure S3. TGA/DTA/MS curves and the evolution of gases for LCoH-DS 4.

The measurement was performed in a synthetic air atmosphere (flow rate 30 mL min⁻¹) from 30 to 1100 °C with a heating rate of 5 °C min⁻¹.

The thermal behaviour of all the prepared samples is similar.

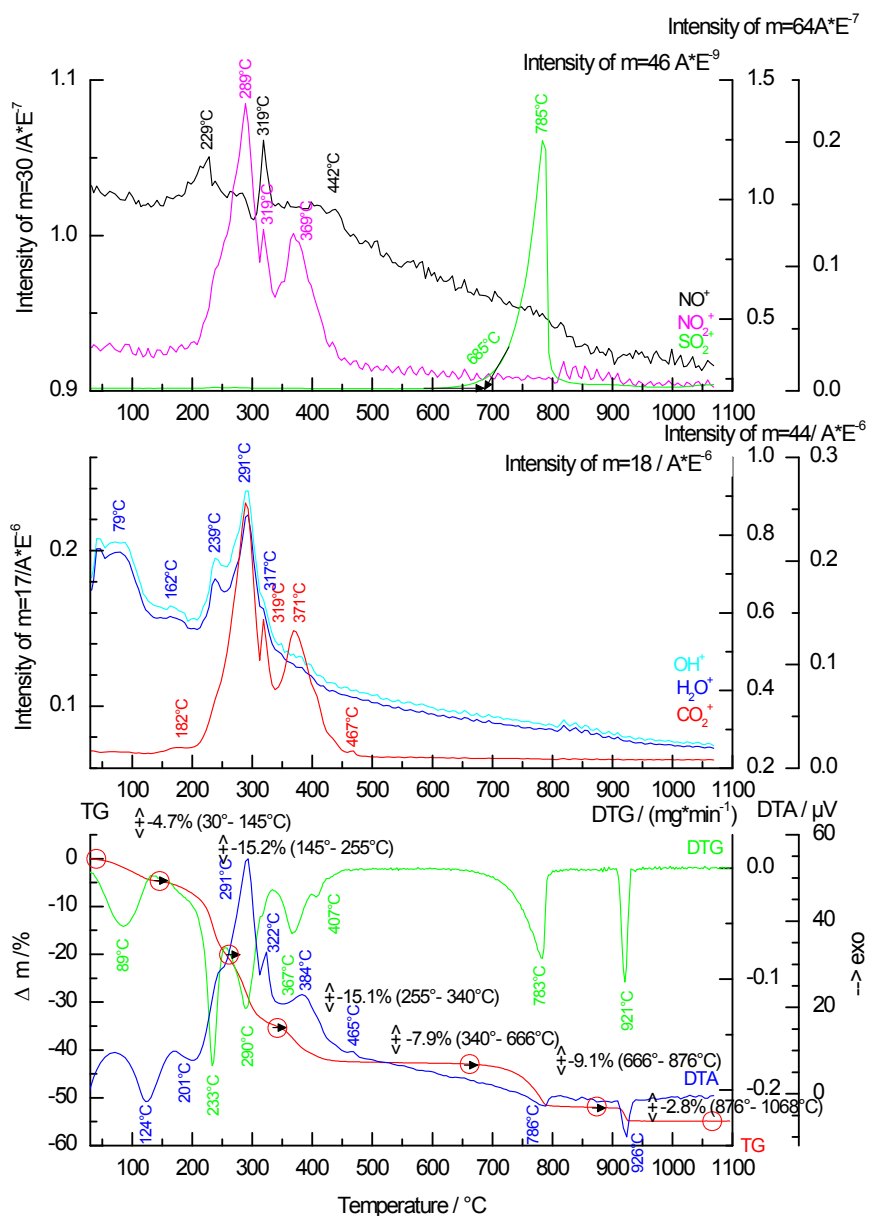


Figure S4. TGA/DTA curves for LCoH-Lactate.

The measurement was performed in a synthetic air atmosphere (flow rate 30 mL min⁻¹) from 30 to 1100 °C with a heating rate of 5 °C min⁻¹.

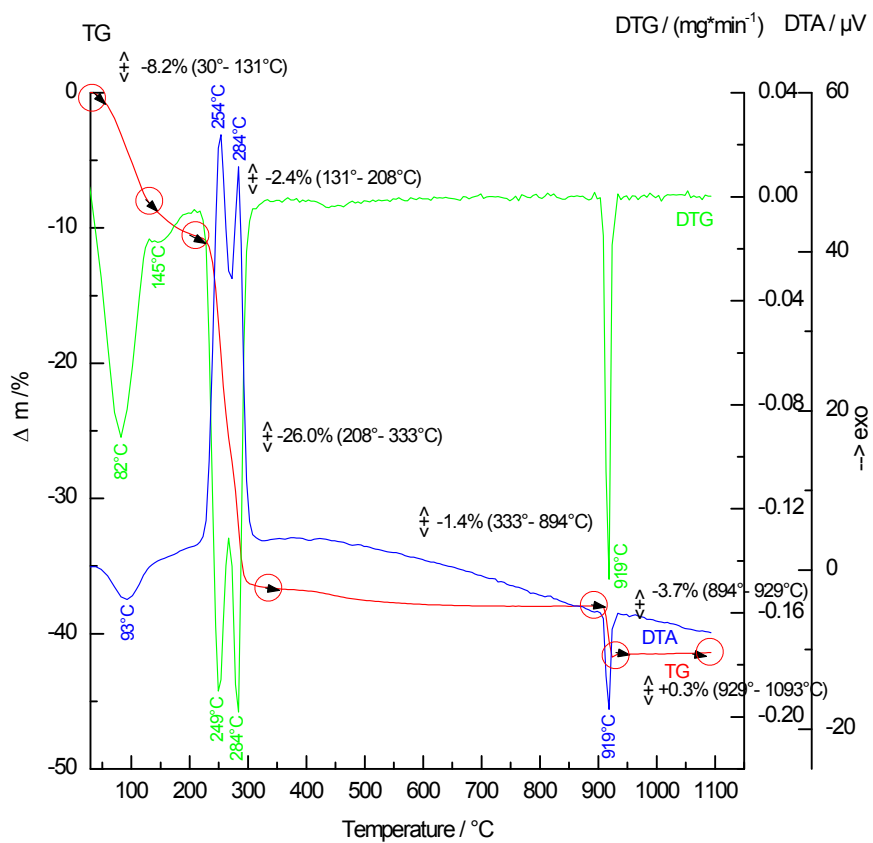


Figure S5. UV/vis absorption spectra of the LCoH-Lactate dispersion (a) and self-standing film (b). Spectra are vertically shifted.

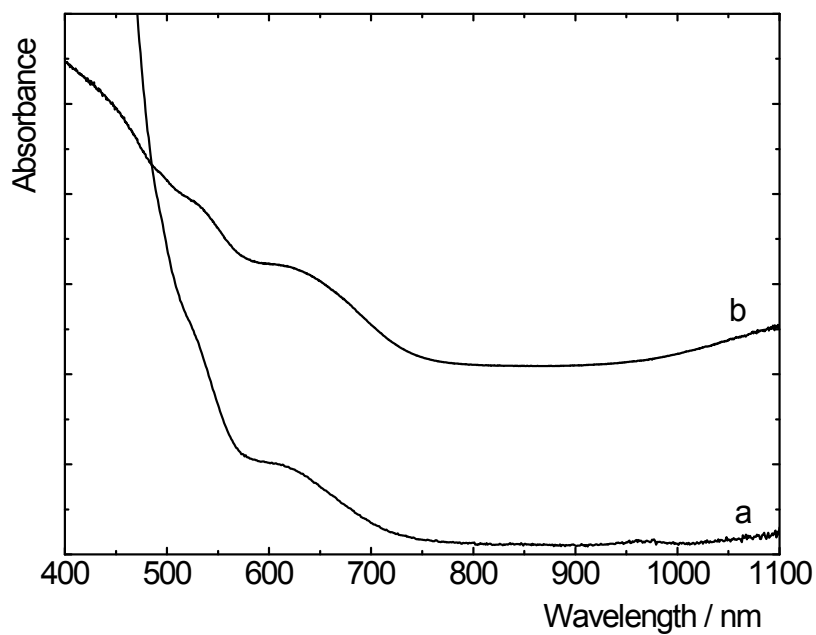


Figure S6. SAXS curves of the aqueous nanosheet dispersions were corrected for scattering from an empty capillary and solvent, intraparticle interference, and were normalized to unit concentration ($1 - 4 \text{ mg mL}^{-1}$).

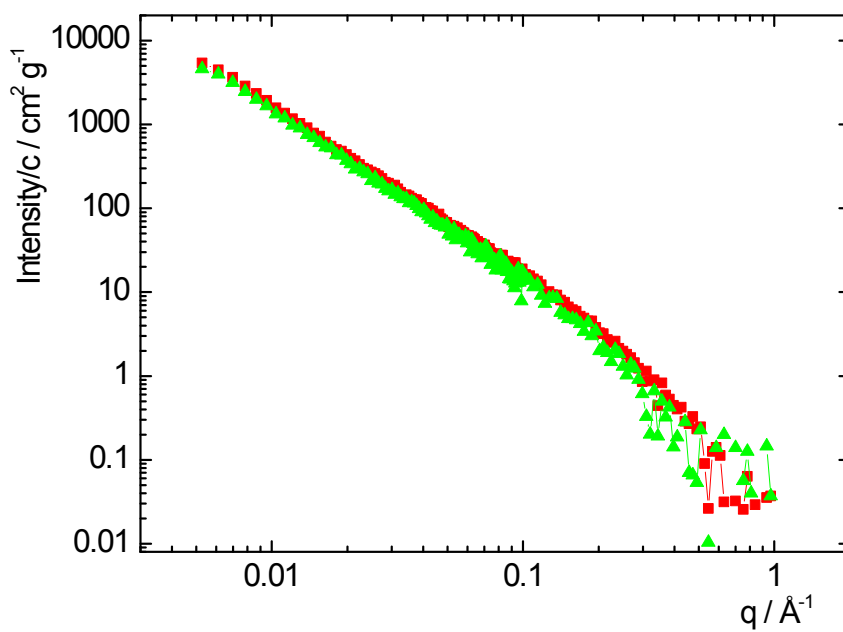


Figure S7. SAXS curve of the aqueous LCoH-Lactate dispersion (4 mg mL^{-1}). The red curve is a fitting scattering function of a model planar particle.

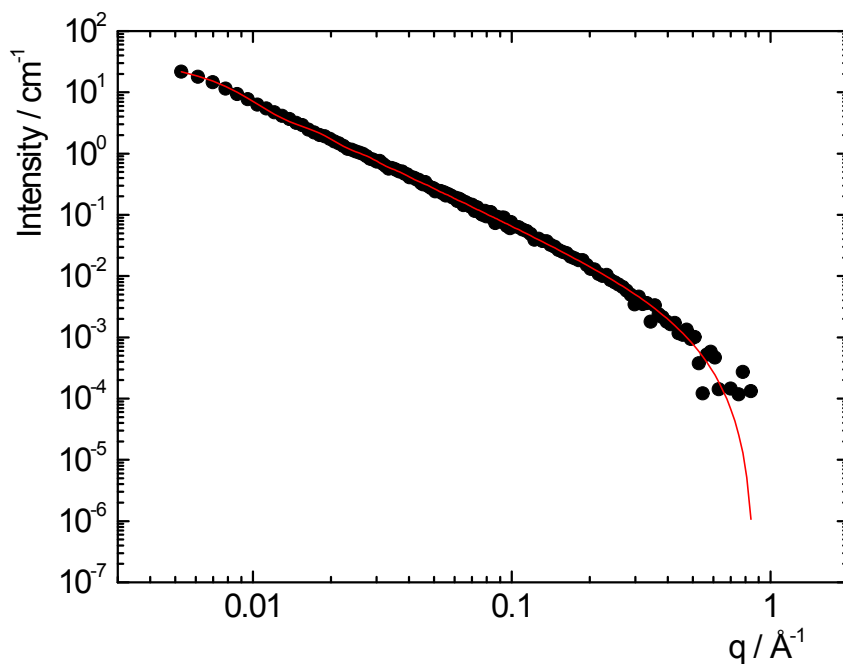


Figure S8. (A) AFM amplitude image (tapping mode) of the drop-casted deposit on the basal plane HOPG that was prepared from the aqueous dispersion of the LCoH-Lactate nanosheets (2 mg mL^{-1}); (B) the same after repetitive potential cycling (from -800 mV to $+500 \text{ mV}$ vs. SCE) in aqueous 1 M KOH solution.

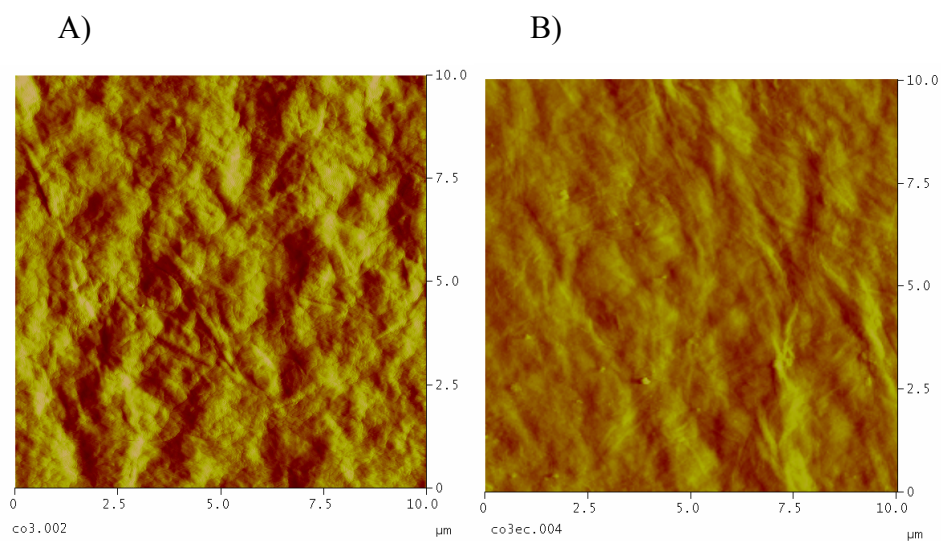


Figure S9. Dependence of the peak current (I_a is the anodic peak current; I_c is the cathodic peak current) vs. potential scan rate (v) for the spin-coated cobalt hydroxide deposits on HOPG. Measurements (A) and (B) represent the deposits prepared using 10 and 2 mg mL⁻¹ nanosheet dispersions, respectively.

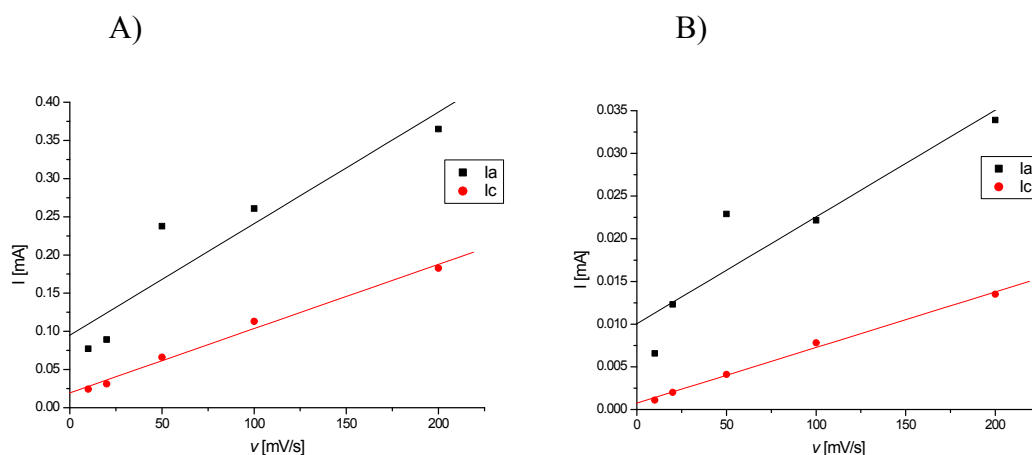


Figure S10. Dependence of the peak potential (E_a is the anodic peak potential; E_c is the cathodic peak current) vs. potential scan rate (v) for the spin-coated cobalt hydroxide deposits on the basal plane HOPG. Measurements (A) and (B) represent the deposits prepared using 10 and 2 mg mL⁻¹ nanosheet dispersions, respectively. Potentials are related to the saturated calomel reference electrode (SCE).

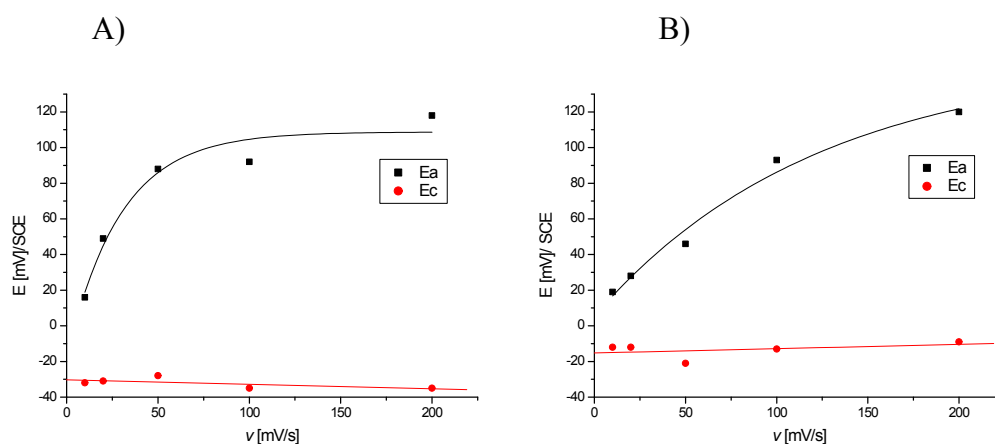


Figure S11. Cyclic voltammetry of the spin-coated nanosheet deposits on the basal plane HOPG. Voltammetry was performed in aqueous 1 M KOH electrolyte deoxygenated with Ar. Scan rate was 100 mV s⁻¹. Measurements (A) and (B) represent the deposits prepared using 10 and 2 mg mL⁻¹ dispersions, respectively. The potentials are related to SCE.

